The role of stress transfer in earthquake occurrence

Ross S. Stein

US Geological Survey, MS 977, Menlo Park, California 94025, USA

An earthquake alters the shear and normal stress on surrounding faults. New evidence strengthens the hypothesis that such small, sudden stress changes cause large changes in seismicity rate. Rates climb where the stress increases (aftershocks) and fall where the stress drops. Both increases and decreases in seismicity rate are followed by a time-dependent recovery. When stress change is translated into probability change, seismic hazard is seen to be strongly influenced by earthquake interaction.

During the 75 years before the great 1906 earthquake on the San Andreas fault, the San Francisco Bay area suffered at least 14 shocks of moment magnitude (M_w) equal to or exceeding 6; these occurred on all major faults, and included two events of $M_w \geq 6.8$. In the succeeding 75 years, there was but one $M_w \geq 6$ shock[1] (Fig. 1). Elsewhere, $M_w \geq 6$ earthquakes in the extensional regime seaward of subduction zones occur, with few exceptions, only in the years following great subduction events[2]. Evidently, the rate of seismicity is therefore not constant, and the rate—or probability—of earthquakes on one fault is not independent of the rate on another. Yet there is nothing in probabilistic seismic hazard assessment (the principal tool of the engineering, insurance, financial, and emergency-response communities) that reflects or can reproduce such observations. Earthquake interaction is a fundamental feature of seismicity, leading to earthquake sequences, clustering, and aftershocks. One interaction criterion that promises a deeper understanding of earthquake occurrence, and a better description of probabilistic hazard, is Coulomb stress transfer.

Coulomb failure stress

An earthquake reduces the average value of the shear stress on the fault that slipped, but as Chinnery first showed in 1963, shear stress rises in more areas than just the fault tips[3]. The importance of this discovery was realized about 20 years later, when lobes of off-fault aftershocks were seen to correspond to small calculated increases in shear[4] or Coulomb stress[5,6]. In its simplest form, the Coulomb failure stress change, $\Delta\sigma_f$ (also written ΔCFS or ΔCFF) is

$$\Delta\sigma_f = \Delta\tau + \mu(\Delta\sigma_n + \Delta P) \quad (1)$$

where $\Delta\tau$ is the shear stress change on a fault (reckoned positive in the direction of fault slip) and $\Delta\sigma_n$ is the normal stress change (positive if the fault is unclamped). ΔP is the pore pressure change in the fault zone (positive in compression), and μ is the friction coefficient (with range 0–1). Failure is encouraged if $\Delta\sigma_f$ is positive and discouraged if negative; both increased shear and unclamping of faults promote failure. The tendency of ΔP to counteract $\Delta\sigma_n$ is often incorporated into equation (1) by a reduced 'effective' friction coefficient, μ' (ref. 7).

The calculated off-fault stress increases are rarely more than a few bars (1 bar = 0.1 MPa, which is approximately atmospheric pressure at sea level), or just a few per cent of the mean earthquake stress drop. In addition, the proximity to failure at any site is presumably variable but in any event unknown. So why would aftershocks concentrate at the site of such small stress increases? New studies

Figure 1 Comparison of earthquakes before and after the $M_w = 7.8$ San Francisco earthquake on the San Andreas fault. Solid red lines, interpreted rupture positions[42]; dashed red lines, the 1906 earthquake. Urban areas are shown grey. S.F. Bay, San Francisco Bay. Although this is the longest historical earthquake record in the western United States, it is probably complete for $M_w \geq 6$ only since the 'gold rush' of 1849, and so underestimates the rate of shocks during the pre-1906 period. The southern end of the 1906 rupture lies near the bottom of the image; the northern end lies 200 km northwest of the image. Processing by R. E. Crippen.

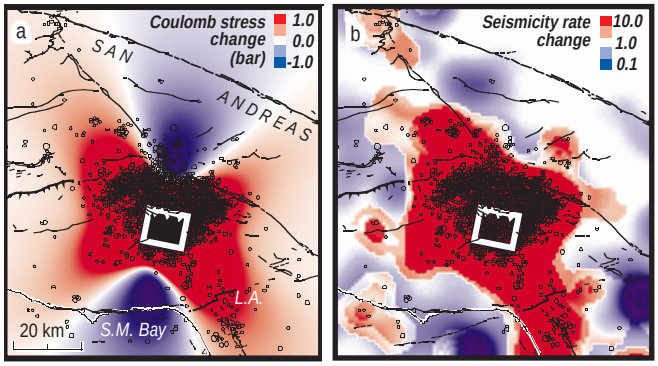

Figure 2 Correlation between calculated Coulomb stress change and seismicity rate change for the 1994 $M_w = 6.7$ Northridge earthquake. **a**, The largest Coulomb stress change on optimally oriented thrust or strike-slip faults at depths of 3–10 km; the compressive axis of the regional stress is oriented N4° E, and $\mu = 0.4$ (ref. 43). Locations of active surface faults, and $M_w \geq 1.5$ shocks during 3–6 months after the mainshock, are superimposed in black. **b**, The seismicity rate change (new/old), comparing the rate during the 78 months before the Northridge earthquake to that 3–6 months afterwards[44] (the first 3 months after Northridge have a poorer level of completeness and are excluded). The rate is calculated in 10-km cells on a grid with 1-km spacing and then smoothed with a gaussian filter. The rate change in the white areas is unresolved. About 65% of the resolved area is positively correlated. Such correlations extend 40 km (or 4 fault lengths) southeast of the mainshock to Los Angeles (L.A.). Observed seismicity rate decreases in the Santa Monica Bay (S.M. Bay) and along parts of the San Andreas fault are correlated with the calculated stress decrease.

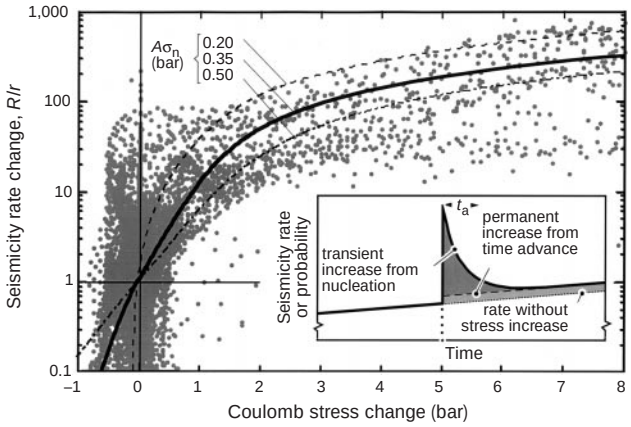

Figure 3 Observed seismicity rate change as a function of calculated Coulomb stress change for the 1995 $M_w = 6.9$ Kobe earthquake[34]. Main figure, seismicity rate change for $M_w \geq 2.6$ earthquakes (the minimum magnitude for which the catalogue is complete) during 8 years before the Kobe shock compared to the following 1.5 years; the seismicity rate increased after the Kobe earthquake where the rate change $R/r > 1$ and fell where $R/r < 1$. The maximum Coulomb stress change on optimally oriented strike-slip and thrust faults is calculated at depths of 0–20 km, for $\mu = 0.4$. Inset, schematic illustration of the time-dependence of seismicity rate (graphically similar to conditional earthquake probability), following a sudden stress increase; the transient effect of the stress increase decays to the permanent rate change over the aftershock duration, t_a (refs 33, 34). $A\,\sigma_n$ is the product of the state/rate constitutive parameter A (ref. 30) and the total normal stress acting on the fault, σ_n.

find a surprisingly strong influence of stress change on seismicity, and seek to explain it in terms of rupture nucleation phenomena observed in the laboratory.

Stress change and seismicity rate change

More than any other earthquake, the 1992 $M_w = 7.3$ shock in Landers, California, changed the landscape of stress-triggering investigations. Rich in aftershocks, this well-recorded event enabled detailed estimates to be made of the distribution of the fault slip, needed to calculate the stress changes. Because in map view the strike-slip rupture is concave to the west, the earthquake was calculated to produce a 2-bar lobe of Coulomb stress increase 40 km west of the mainshock, where the $M_w = 6.5$ Big Bear shock struck 2.5 hours after Landers[8]. While this association alone could result from chance, 67% of the 10,000 $M > 1$ Landers–Big Bear aftershocks also occurred in regions calculated to have been brought >0.1 bar closer to failure (termed the stress-triggering zones), and few off-fault aftershocks occurred in regions inhibited by >0.1 bar from failure (the stress shadows)[7,9–11]. Most of these comparisons of stress change to aftershocks rely on the assumption that small shocks occur on planes optimally oriented for failure as a result of the regional stress and the earthquake stress change[7]. The association of calculated Coulomb stress increases with aftershocks is now widely reported (see ref. 12 and references therein).

Tantalizing as it may be, finding aftershocks in the stress trigger zones does not demonstrate that the stress imparted by the mainshock had any effect on off-fault seismicity, as seismicity may have been as abundant in those zones before the mainshock. A stronger test of the Coulomb hypothesis is to compare the calculated stress change to the observed seismicity rate change[13]. After a mainshock, sites of both increased *and* decreased seismicity rate are seen; for the $M_w = 6.7$ 1994 Northridge, California, shock, 65% of the observed seismicity rate changes are correlated with the calculated Coulomb stress change (Fig. 2).

An earthquake can thus enhance or suppress subsequent events, depending on their location and orientation. Viewed in this light, aftershocks are simply sites of seismicity rate increase, occurring where the stress has increased—whether on the fault rupture or off. Sites of seismicity rate decrease, or where the rate was higher before the earthquake than after, might logically be called 'antishocks' (in the sense of '*antipasto*'—they precede rather than follow the main course). A spatial regression of stress change on seismicity rate change for the 1995 $M_w = 6.9$ Kobe, Japan, earthquake (Fig. 3, main panel) reveals just how strong this effect is: a 1-bar stress increase corresponds to a 10-fold increase in rate of shocks with local magnitude $M_L \geq 2.6$; a 5-bar stress change is associated with a 100-fold rate increase. But are such findings valid if small aftershocks, whose nodal planes are unknown, do not occur on faults optimally oriented for failure? One alternative is to consider only seismicity on (say, within 1 km of) major active faults and assume that these shocks have the same strike, dip and rake as the fault on which they occur. Another approach is to calculate the Coulomb stress change on the nodal planes of the subset of shocks with known focal mechanisms. Both approaches yield new insights, as outlined below.

Several researchers[13–15] have examined stress changes and seismicity on major faults within 100 km of the 1989 $M_w = 6.9$ Loma Prieta, California, shock. Parsons *et al.*[15] found that the seismicity rate change is associated with the calculated shear stress change for major faults (slip rates more than ~7 mm yr^{-1} and cumulative slip of more than ~50 km; Fig. 4a). For minor faults (with negligible cumulative slip and lower slip rates—typically thrust or oblique faults), seismicity is concentrated where the faults were unclamped (Fig. 4b); both correlations are statistically significant. Restated in terms of equation (1), the effective friction coefficient on the major faults is low ($\mu' \leq 0.2$), while for minor faults it is high ($\mu' \geq 0.8$). This inference accords with independent arguments that major faults such as the San Andreas develop thick, impermeable gouge zones that reduce sliding friction or trap pore fluids[16,17], both of which lower μ'. The 1997 sequence of eight shocks, all of $M_w = 5$–6, that occurred in Umbria-Marche, Italy, on normal faults with low slip rates and modest net slip, also appears to have been promoted by unclamping[18]. Seeber and Armbuster[19] found that the ratio of encouraged to discouraged aftershocks of the Landers earthquake is

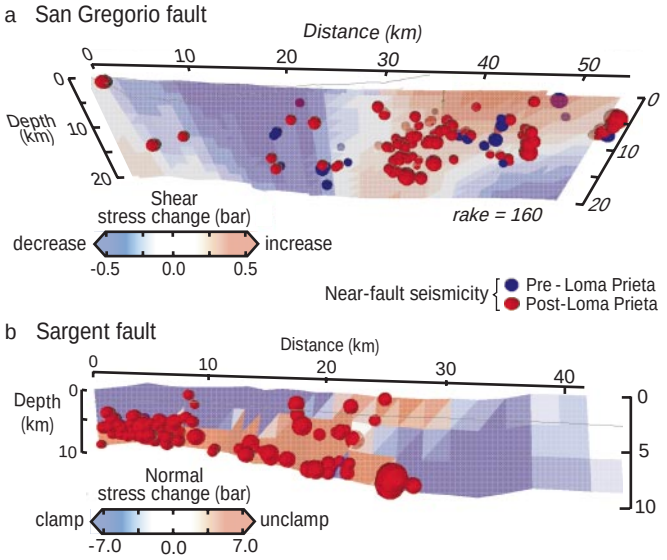

Figure 4 Seismicity and stress changes associated with the 1989 $M_w = 6.9$ Loma Prieta earthquake resolved on nearby faults[15]. Fault locations are shown in Fig. 6a. Seismicity with $M_L \geq 1.5$ during 7 years before and after Loma Prieta is plotted, with size proportional to magnitude. Distance increases towards the southeast. **a**, The fault is assumed to dip 70° northeast with a 160° rake, consistent with focal mechanisms and marine terrace deformation; the thin line is the coast. Earthquakes within 2 km of the fault are shown. The change in the seismicity distribution is associated with the calculated shear stress change, suggesting that μ is low (no correlation is seen for normal stress change). **b**, The fault is assumed to dip 55 ± 5° southwest and has a 135° rake; the thin line is the surface projection of the San Andreas fault. Earthquakes within 1 km of the fault are shown. The post-1989 seismicity is concentrated where the fault was unclamped, suggesting a high μ (no correlation is seen for shear stress change).

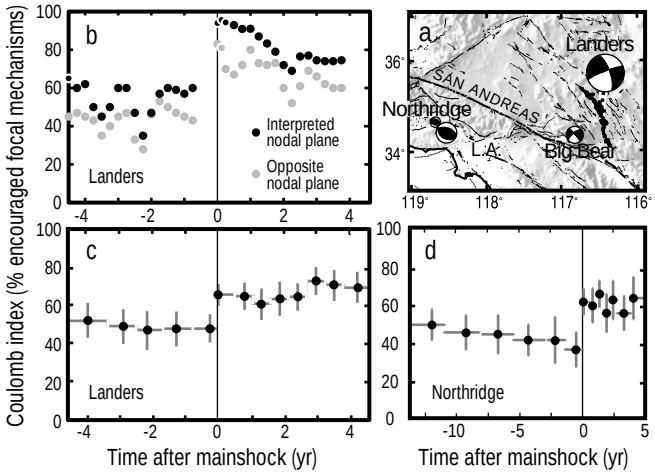

Figure 5 Stress changes associated with the 1992 $M_w = 7.3$ Landers and the 1994 $M_w = 6.7$ Northridge ruptures resolved on nodal planes of earthquakes with focal mechanisms. The percentage of planes brought closer to failure ('encouraged') is ~50% by chance before the main ruptures, but increases significantly afterwards, indicating that aftershocks tend to occur where the main rupture has promoted Coulomb failure. **a**, Focal mechanisms of the mainshock and largest aftershock in both sequences; LA, Los Angeles. **b**, $M_L \geq 1.5$ shocks ≥27 km from the Landers rupture are used, at sites where the calculated stress change is ≥0.2 bar, assuming that $\mu = 0.85$ (ref. 19). **c**, $M_L \geq 2.5$ shocks within a box defined by 32.5–36.5° N/115.5–119.5° W are included, assuming $\mu = 0.4$ (ref. 20); 95% confidence bounds are shown. Events with both planes encouraged receive more weight than those with one encouraged plane. **d**, $M_L \geq 2.5$ shocks within a box defined by 33.8–34.9° N/117.8–119.5° W, assuming $\mu = 0.4$ (ref. 45); 95% confidence bounds shown.

greatest if $\mu' = 0.85$; minor faults surround Landers. Thus the high friction inferred for minor faults seems to be borne out by several Coulomb studies.

Using focal mechanisms to evaluate the Coulomb hypothesis affords additional insights but presents new problems, because the Coulomb stress change is different on the two nodal planes of the focal mechanism, unless $\mu = 0$. Hardebeck *et al.*[20] calculated the Coulomb stress change on both planes, and examined whether the percentage of encouraged planes increases after the Landers and the Northridge earthquakes (Fig. 5a); the period before the earthquakes served as a control group. The 20–25% increase in the percentage of encouraged shocks (Fig. 5c and d) is statistically significant for stress increases ≥0.1 bar, and persists for the 5 years examined after both mainshocks. Seeber and Armbruster[19] interpreted the fault plane for each of the 1900 aftershock focal mechanisms of Landers, and reached similar conclusions, although they found a larger initial increase in encouraged aftershocks that decays with time (Fig. 5b). A test for aftershocks of the 1987 $M_w = 6.6$ sequence at Superstition Hills, California, also shows significant correlations for stress increases ≥0.1 bar during 1.4–2.8 yr after the mainshock[21].

Dynamic and tidal Coulomb stress change

The seismic waves excited by earthquakes produce dynamic Coulomb stress changes that, at distances more than about one source dimension from the fault, can be an order of magnitude larger than the static stress changes. How can one distinguish whether the static or dynamic stresses control seismicity? In other words, is it strong shaking or the weak permanent stress changes that promote seismicity? Because the dynamic stresses oscillate, they are everywhere positive at some point in time. All sites are shaken, and thus the dynamic stresses cast no stress shadows and should produce no 'antishocks' (seismicity rate decreases), at odds with observations. Belardinelli *et al.*[22] calculated the dynamic stress evolution in the 1980 $M_w = 6.9$ Irpinia, Italy, sequence in which nearby faults ruptured 20 s apart. The second event was not triggered at the time of the dynamic peak. Rather, a delayed triggering mechanism must be involved irrespective of whether static or dynamic stresses are responsible, because the second rupture nucleated 12 s after the dynamic peak and 6 s after the static value had been reached.

Other evidence, however, suggests that at larger distances from the rupture, dynamic stresses may explain the distribution of seismicity rate changes better than the static stresses. Kilb *et al.*[23] found that the pattern of dynamic Coulomb stress changes bears similarities to that for static stress changes. Although the peak dynamic stress field lacks shadows, it does exhibit lobes with small stress change in roughly the same positions as the static stress shadows. The vital difference is that the dynamic stress increases are an order of magnitude larger in the direction of rupture propagation. The Landers rupture propagated unilaterally to the northwest, and produced more aftershocks in this direction[24]. The observed seismicity rate may thus be influenced by both static and dynamic effects.

If static stress changes influence earthquake occurrence, then seismicity rates might be modulated by the solid Earth tides, the distortion of the Earth caused by the pull of the Sun and Moon. Unlike earthquakes, the tides produce no strong motion (shaking), but they do alter the stress on faults. The tidal Coulomb stress range, dominated by the normal-stress component, is only about ±0.01 bar, or one-tenth of the threshold of detection in the most sensitive aftershock studies. Vidale *et al.*[25] calculated the tidal stresses on the fault planes of 13,000 earthquakes along the creeping portions of the San Andreas and Calaveras faults, and found that the seismicity rate is higher at times when the tidal stresses unclamped the fault, but not significantly so. Lockner and Beeler[26] cycled stress

in a laboratory sample to simulate the tides, and found that stress changes ⩾0.1 bar caused strong correlations in the timing of stick-slip events, in accord with aftershock studies. They estimated that if detection increased with the square root of the sample size, more than 20,000 earthquakes would be needed to find a statistically significant association with tidal stresses, in which case ~1.5% of the seismicity would be correlated. Vidale *et al.*[27] repeated their experiment with 27,500 quakes, and found that the rate of seismicity during the peak tidal unclamping is 1.0% higher than average, a difference significant at the 95% confidence level. Thus the tides perceptibly alter the rate of seismicity, suggesting that the much larger off-fault stress changes associated with earthquakes are indeed one cause of seismicity rate changes.

Incorporating stress transfer into probabilistic hazard

The simplest way to incorporate stress transfer into probability models is to assume that a sudden stress change will alter the time until the next large earthquake by the ratio of the stress change on the fault to its long-term stressing rate. This is the 'time advance or delay' used in some consensus probability forecasts[28,29]. Because stress changes on nearby faults are typically of the order 1 bar, and stressing rates are of the order 0.1 bar yr^{-1}, inter-event times are only changed by decades. Such a time change is inevitably much smaller than the uncertainty or variability of the earthquake inter-event time (typically assigned to be ±50%), and thus has little effect on the probability. But why, then, would earthquake stress changes exert such a strong influence on seismicity rates? The 1906 stress decrease on the faults in the San Francisco Bay area, for example, is a few bars, but the rate of $M_w \geqslant 6$ shocks dropped by at least an order of magnitude during the ensuing 75 years (Fig. 1), in a manner consistent with the Kobe results (Fig. 3a).

A way out of this problem is suggested by the concept of state and rate friction. The observed dependence of seismicity rate on Coulomb stress change (Fig. 3, main panel) is well described by Dieterich's earthquake-rate relation[30,31]. In state and rate friction, seismicity is viewed as a sequence of independent nucleation events in which the 'state' depends on the fault slip, slip rate, and elapsed time since the last event. In the absence of a stress perturbation, the seismicity rate is constant. But under the assumption that there is a large number of earthquake nucleation sites on the fault, there is a nonlinear dependence of the time to instability on stress change. The 'time advance' causes a modest but permanent increase in earthquake rate and probability. The transient effect of the stress change strongly amplifies the permanent change, because the fault slips at a higher rate, causing a higher rate of earthquake nucleation (Fig. 3, inset). The transient effect decays as the supply of nucleation sites is consumed; the duration of the transient is inversely proportional to the fault stressing rate.

The seismicity rate equation[30] in simplest form is

$$R(t) = \frac{r}{\left[\exp\left(\frac{-\Delta\sigma_f}{A\sigma_n}\right) - 1\right]\exp\left(\frac{-t}{t_a}\right) + 1} \qquad (2)$$

in which R is the seismicity rate as a function of time, t, following a Coulomb stress change, $\Delta\sigma_f$. A is a constitutive parameter, σ_n is the total normal stress, t_a is the aftershock duration (equal to $A\sigma_n/\dot{\tau}$, where $\dot{\tau}$ is the stressing rate on the fault), and r is the seismicity rate before the stress perturbation. To evaluate equation (2), the Coulomb stress change is calculated and r, t_a and $\dot{\tau}$ are estimated from observations, permitting $A\sigma_n$ to be inferred (Fig. 3, main panel).

The rate equation (equation (2)) has the form of Omori's law, which describes the observed temporal decay of aftershocks on the mainshock rupture surface. Thus the decay of seismicity following a stress change may instead be a general property of earthquakes, restricted neither to aftershocks nor to the rupture surface. Such an interpretation is borne out by observations: even at distances more than 40 km from the Loma Prieta fault—well outside the traditional aftershock zone—the response to a stress change of either sign is a sudden seismicity rate change followed by a recovery roughly to the former rate[32] (Fig. 6). The close resemblance between the observed behaviour of seismicity following such a stress increase (Fig. 6b) and that modelled with equation (2) (Fig. 3, inset) is evident.

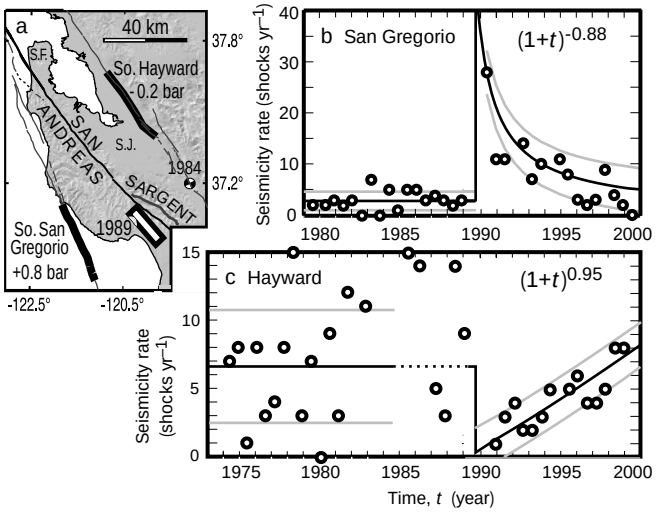

Figure 6 The influence of stress changes associated with the Loma Prieta earthquake on $M_L \geqslant 1.5$ seismicity rates[32]. Such influence is found well outside what is traditionally regarded as the aftershock zone. **a**, Map of Loma Prieta source (rectangle) and Southern Hayward and southern San Gregorio fault sections (bold) on which stress change is calculated and seismicity rates are measured: S.F. is San Francisco; S.J. is San Jose. **b**, Seismicity rate jumps on the southern San Gregorio fault, 40 km west of Loma Prieta. The 95% confidence limits for the pre-1989 rate and the post-1989 decay are shown by the thin grey lines. The decay obeys Omari's law (see text); the aftershock duration, t_a = 5–28 yr at 95% confidence. **c**, Seismicity rate drops on the southern Hayward fault, 40–80 km north of Loma Prieta, and then recovers during the following ~8 years. (Some 30 km southeast of the south Hayward fault, the 1984 M_w = 6.2 Morgan Hill shock disrupts the seismicity during 1984–88, so this period is not used to estimate the pre-1989 seismicity rate. The highest values exceed 20 shocks yr^{-1} during this period.)

Although, for small shocks, seismicity rate changes and probabilities can be tested against observations, the calculated probabilities for large earthquakes are more difficult to validate because there are so few large shocks. Probability calculations are also fraught with uncertainties associated with the prospective earthquake's location and magnitude, the variation of the earthquake inter-event time, and the probability density function (how the probability grows with time). Monte Carlo simulation can capture the range of behaviour, but this range can be frustratingly large. But the probability changes associated with earthquake transfer are less sensitive to these assumptions, enabling inferences to be made about how the probability of an earthquake on one fault is affected by a nearby large earthquake on another.

Several attempts to estimate earthquake probabilities using stress transfer and state and rate friction have been made. The seven $M_w \geqslant 6.8$ 'falling-domino' shocks on the North Anatolia fault during 1939–67 are obvious candidates, because it is difficult to explain such a rapid and progressive sequence unless transient probability gains associated with stress transfer are included. In 1997, my colleagues and I calculated that there was an average 3-fold probability gain at the site of each successive event caused by the preceding earthquakes[33]. We also identified two segments—two dominoes still standing—where the stress rise since 1939 was greatest. We calculated a 15% 30-year probability for a large earthquake near Erzincan, a 12% probability near Izmit, but only a <1% probability on the remaining 750 km of the fault. The 17 August

1999 $M_w = 7.4$ Izmit shock occurred in one of these stressed sites. The Izmit earthquake, in turn, increased the Coulomb stress and rate of seismicity on the Düzce fault, located east of the August rupture, and the Yalova fault, located west of the August rupture[46]. The 12 November 1999 $M_w = 7.2$ Düzce earthquake subsequently struck on the Düzce fault where the stress was increased by ~3 bar.

Japan and California have proved to be important sites for testing such interaction-based probabilities. Toda *et al.*[34] calculated a 10-fold probability drop during the next 30 years on the section of the major fault most discouraged from failure by the 1995 $M_w = 6.9$ Kobe shock, and a 5-fold probability gain on the section most stressed, which lies near Kyoto. Three studies have focused on the San Francisco Bay area where, as in the other cases, the consequences of an urban $M_w = 7$ shock loom large, but the interaction of several sub-parallel faults is simpler than in Japan. Building on the stress analysis of Jaumé and Sykes[35], Harris and Simpson[36] retrospectively evaluated the suppression of $M_w \geqslant 6$ shocks in the San Francisco Bay area after 1906, finding the set of stress and state/rate constitutive parameters consistent with the observed rate change. Prospective studies of the probability of a $M_w = 6.8$ shock on the Hayward fault during 2000–30, such as occurred in 1868, find that the probability is 15–25% lower if the effect of the 1906 shock is included[32,37].

These nascent probability calculations are faithful to the presence of aftershocks, the characteristics of large earthquake sequences, the change in location and style of upper-plate earthquakes following subduction events[38], and the cessation of large shocks in the San Francisco Bay area after 1906. Perhaps most surprising, one finds that the stress trigger or shadow cast by a great earthquake can exert an influence on earthquake occurrence for more than a century. What lies ahead is fuller incorporation of viscoelastic[39–41] and poroelastic effects that modify the Coulomb stress with time, real-time tests of earthquake rate and probability calculations, and further exploration of seismicity rate changes and the dynamic Coulomb stresses. □

1. Bakun, W. H. Seismic activity of the San Francisco Bay region. *Bull. Seismol. Soc. Am.* **89,** 764–784 (1999).
2. Lay, T., Astiz, L., Kanamori, H. & Christensen, D. H. Temporal variation of large interplate earthquakes in coupled subduction zones. *Phys. Earth Planet. Inter.* **54,** 258–312 (1989).
3. Chinnery, M. A. The stress changes that accompany strike-slip faulting. *Bull. Seismol. Soc. Am.* **53,** 921–932 (1963).
4. Das, S. & Scholz, C. H. Off-fault aftershock clusters caused by shear stress increase? *Bull. Seismol. Soc. Am.* **71,** 1669–1675 (1981).
5. Stein, R. S. & Lisowski, M. The 1979 Homestead Valley earthquake sequence, California: Control of aftershocks and postseismic deformation. *J. Geophys. Res.* **88,** 6477–6490 (1983).
6. Oppenheimer, D. H., Reasenberg, P. A. & Simpson, R. W. Fault plane solutions for the 1984 Morgan Hill, California, earthquake sequence: Evidence for the state of stress on the Calaveras fault. *J. Geophys. Res.* **93,** 9007–9026 (1988).
7. King, G. C. P., Stein, R. S. & Lin, J. Static stress changes and the triggering of earthquakes. *Bull. Seismol. Soc. Am.* **84,** 935–953 (1994).
8. Stein, R. S., King, G. C. P. & Lin, J. Change in failure stress on the southern San Andreas fault system caused by the 1992 magnitude = 7.4 Landers earthquake. *Science* **258,** 1328–1332 (1992).
9. Harris, R. A. & Simpson, R. W. Changes in static stress on southern California faults after the 1992 Landers earthquake. *Nature* **360,** 251–254 (1992).
10. Jaumé, S. C. & Sykes, L. R. Change in the state of stress on the southern San Andreas fault resulting from the California earthquake sequence of April to June 1992. *Science* **258,** 1325–1328 (1992).
11. Gross, S. & Kisslinger, C. Estimating tectonic stress rate and state with Landers aftershocks. *J. Geophys. Res.* **102,** 7603–7612 (1997).
12. Harris, R. A. Introduction to special session: Stress triggers, stress shadows, and implications for seismic hazard. *J. Geophys. Res.* **103,** 24347–24358 (1998).
13. Reasenberg, P. A. & Simpson, R. W. Response of regional seismicity to the static stress change produced by the Loma Prieta earthquake. *Science* **255,** 1687–1690 (1992).
14. Simpson, R. W. & Reasenberg, P. A. in *The Loma Prieta, California, Earthquake of October 17, 1989—Tectonic Processes and Models* (ed. Simpson, R. W.) F55–F89 (Professional Paper 1550-F, US Geological Survey, 1994).
15. Parsons, T., Stein, R. S., Simpson, R. W. & Reasenberg, P. A. Stress sensitivity of fault seismicity: A comparison between limited-offset oblique and major strike-slip faults. *J. Geophys. Res.* **104,** 20183–120202 (1999).
16. Zoback, M. D. *et al.* New evidence on the state of stress of the San Andreas fault system. *Science* **238,** 1105–1111 (1987).
17. Rice, J. R. in *Fault Mechanics and Transport Properties of Rock* (eds Evans, B. & Wong, T.-F.) 475–504 (Academic, London, 1992).
18. Cocco, M., Nostro, C. & Ekström, G. Static stress changes and fault interaction during the 1997 Umbria-Marche earthquake sequence. *J. Geophys. Res.* (in the press).
19. Seeber, L. & Armbruster, J. G. Earthquakes as beacons of stress change. *Nature* (submitted).
20. Hardebeck, J. L., Nazareth, J. J. & Hauksson, E. The static stress change triggering model: Constraints from two southern California aftershocks sequences. *J. Geophys. Res.* **103,** 24427–24437 (1998).
21. Anderson, G. & Johnson, H. A new statistical test for static stress triggering: Application to the 1987 Superstition Hills earthquake sequence. *J. Geophys. Res.* **104,** 20153–20168 (1999).
22. Belardinelli, M. E., Cocco, M., Coutant, O. & Cotton, F. Redistribution of dynamic stress during coseismic ruptures: Evidence for fault interaction and earthquake triggering. *J. Geophys. Res.* **104,** 14925–14946 (1999).
23. Kilb, D., Gomberg, J. & Bodin, P. Aftershock triggering by dynamic and static Coulomb stress changes. *Eos (suppl.)* **79,** F647 (1998).
24. Hill, D. P. *et al.* Seismicity remotely triggered by the magnitude 7.3 Landers, California, earthquake. *Science* **260,** 1617–1623 (1993).
25. Vidale, J. E., Agnew, D. C., Johnston, M. S. J. & Oppenheimer, D. H. Absence of earthquake correlation with earth tides: An indication of high preseismic fault stress rate. *J. Geophys. Res.* **103** (1998).
26. Lockner, D. A. & Beeler, N. M. Premonitory slip and tidal triggering of earthquakes. *J. Geophys. Res.* **104,** 20133–20152 (1999).
27. Vidale, J., Agnew, D., Oppenheimer, D., Rodriquez, C. & Houston, H. A weak correlation between earthquakes and extensional normal stress and stress rate from lunar tides. *Eos (suppl.)* **79,** F641 (1998).
28. Working Group on the probabilities of future large earthquakes in southern California. *Future Seismic Hazards in Southern California, Phase I: Implications of the 1992 Landers Earthquake Sequence* (California Division of Mines & Geology, Sacramento, 1992).
29. Working Group on California earthquake probabilities. Seismic hazards in southern California: Probable earthquakes. 1994–2014. *Bull. Seismol. Soc. Am.* **85,** 379–439 (1995).
30. Dieterich, J. A constitutive law for rate of earthquake production and its application to earthquake clustering. *J. Geophys. Res.* **99,** 2601–2618 (1994).
31. Dieterich, J. H. & Kilgore, B. Implications of fault constitutive properties for earthquake prediction. *Proc. Natl. Acad. Sci. USA* **93,** 3787–3794 (1996).
32. Parsons, T. & Stein, R. Earthquake probabilities in the San Francisco Bay area after 1906: A rate/state approach to fault interactions. *J. Geophys. Res.* (submitted).
33. Stein, R. S., Barka, A. A. & Dieterich, J. H. Progressive failure on the North Anatolian fault since 1939 by earthquake stress triggering. *Geophys. J. Int.* **128,** 594–604 (1997).
34. Toda, S., Stein, R. S., Reasenberg, P. A. & Dieterich, J. H. Stress transferred by the $M_w = 6.5$ Kobe, Japan, shock: Effect on aftershocks and future earthquake probabilities. *J. Geophys. Res.* **103,** 24543–24565 (1998).
35. Jaumé, S. C. & Sykes, L. R. Evolution of moderate seismicity in the San Francisco Bay region, 1850 to 1993: Seismicity changes related to the occurrence of large and great earthquakes. *J. Geophys. Res.* **101,** 765–789 (1996).
36. Harris, R. A. & Simpson, R. W. Suppression of large earthquakes by stress shadows: A comparison of Coulomb and rate-and-state. *J. Geophys. Res.* **103,** 24439–24451 (1998).
37. Reasenberg, P. A., Simpson, R. W., Matthews, M. V., Ellsworth, W. L. & Parsons, T. Recurrence models and fault interactions: an example based on the 1868 Hayward, California, earthquake. *Bull. Seismol. Soc. Am.* (submitted).
38. Taylor, M. A., Dmowska, R. & Rice, J. R. Upper plate stressing and seismicity in the subduction earthquake cycle. *J. Geophys. Res.* **103,** 24523–24542 (1998).
39. Pollitz, F. F. & Sacks, I. S. The 1995 Kobe, Japan, earthquake: A long-delayed aftershock of the offshore 1944 Tonankai and 1946 Nankaido earthquakes. *Bull. Seismol. Soc. Am.* **87,** 1–10 (1997).
40. Freed, A. M. & Lin, J. Time-dependent changes in failure stress following thrust earthquakes. *J. Geophys. Res.* **103,** 24393–24410 (9198).
41. Kenner, S. & Segall, P. Time-dependence of the stress shadowing effect and its relation to the structure of the lower crust. *Geology* **27,** 119–122 (1999).
42. Bakun, W. H. Scenarios for historic San Francisco Bay region earthquakes. *US Geol. Surv. Open File Rep.* **98–785** (1998).
43. Stein, R. S., King, G. C. P. & Lin, J. Stress triggering of the 1994 M = 6.7 Northridge. California, earthquake by its predecessors. *Science* **265,** 1432–1435 (1994).
44. Reasenberg, P. A. Seismicity patterns in southern California before and after the 1994 Northridge earthquake: A preliminary report. *US Geol. Surv. Open-File Rep.* **95–484** (1995).
45. Hardebeck, J. L. & Hauksson, E. Background Stress State Plays a Role in Earthquake Triggering. *Eos (suppl.)* (in the press).
46. Barka, A. The 17 August 1999 Izmit earthquake. *Science* **285,** 1858–1859 (1999).

Acknowledgements

I thank the many colleagues who shared their preliminary research, and R. Dmowska, J. Lin, R. Madariaga, T. Parsons, F. Pollitz, J. Rice and S. Toda for comments. This Review Article was written while at Ecole Normale Supérieure and the Institut de Physique du Globe de Paris. The support of Pacific Gas & Electric Co. is gratefully acknowledged.

Correspondence and requests for materials should be addressed to the author (e-mail: rstein@usgs.gov).